The DOI for this manuscript is doi: 10.1175/2009JAS3263.1

Jet Alignment in a 2 Layer Quasi-Geostrophic Channel Using One-Dimensional Grid Warping.

BRAD E. BEECHLER

Department of Atmospheric and Oceanic Sciences,

University of Colorado, Boulder, Colorado

Cooperative Institute for Research in Environmental Sciences, Boulder, Colorado

NOAA/Earth System Research Laboratory, Boulder, Colorado

JEFFREY B. WEISS

Department of Atmospheric and Oceanic Sciences,

University of Colorado, Boulder, Colorado

GREGORY S. DUANE AND JOSEPH TRIBBIA

National Center for Atmospheric Research, Boulder, Colorado

Submitted *The Journal of the Atmospheric Sciences* July 8, 2009

Revised November 17, 2009

Corresponding author address:

Brad Beechler

NOAA/GSD, Earth Systems Research Lab, Boulder, CO, 80305

Email: brad.e.beechler@noaa.gov

Abstract: Due to position errors traditional methods of data assimilation can broaden and weaken jets or other flow structures leading to reduced forecast skill. Here we develop and test a technique to assimilate properties of coherent structures. Focusing on jets, the technique identifies jets in both the modeled and observed fields and warps the model grid so that the jet positions are better aligned prior to further assimilation of observations. We test the technique using optimal interpolation on the flow in a two-layer quasi-geostrophic channel. The results show that a simple and fast jet position correction algorithm can significantly improve the skill of a 12-hour forecast. Furthermore results indicate that this method of position correction maintains its utility when observations become sparse.

1. Introduction

Current operational data assimilation techniques such as 3DVAR are designed to correct local differences in magnitude between an observed field and a modeled field. These methods do very well in many situations but fall short when a model produces a structure of the correct form but at the wrong location. In the process of correcting magnitudes the form of the modeled structure is degraded in the analysis field that is produced. The goal of this study is to show that it is possible to preserve structures more accurately by implementing a process that will take into account errors in the locations of structures.

Defining error is important when evaluating the predictive skill of a model. Error is commonly calculated from differences in magnitude between a predicted modeled state and an observed state. This intuitive approach can mislead the assessment of a model's skill. One way in which simple definitions of error fail is in errors of location. Models produce structures such as cyclones, storm fronts, and jet streaks, but may not be able to predict all-important characteristics of these structures. Forecast model bias is a persistent problem in numerical modeling and data assimilation (Dee and Silva 1998). For instance Alexander et. al. (1998) show that the MM5 model has trouble accurately predicting the position of cyclones. A complicated structure such as a cyclone can be described using parameters such as the center of the storm's location and velocity, and the cyclone's radius, elongation, and rotational speed (Matyas, 2007). In this study we use the simpler structure of a jet whose characteristics include the location of the jet's maximum velocity and its width. The aspects of a structure that are useful depend on its nature. For example, the jet stream's position is important because it has a large influence on storm tracks and surface temperatures. In fact the jet stream's behavior is so

important that a method to identify the its location and size has been developed for the purpose of describing it's climatology (Koch et al. 2006). For many hazardous weather events it can be argued that the precise location of the event is more important than its specific amplitude. For this reason definitions of error using errors in position have been formulated and used to measure the skills of forecasts and in ensemble-based data assimilation (Hoffman et al., 1995, Nehrkorn et al. 2003, and Lawson and Hansen, 2005). Defining a new measure of error with position differences included leads to increased ability to diagnose position errors and correct them in a model.

While trying to create a method to improve the assimilation of structures it is useful to refer to the most capable assimilator of information that we know of, the human brain, which is very good at finding, labeling, and comparing structures. For instance it would be a simple task for a person to identify the jet stream in a model and its analog in the observed wind patterns. The person might also note that the jet stream that the model is producing is dipping too far into the Great Plains or that this dip is propagating too quickly to the east. A meteorologist would compare the model's prediction with observations and use their experience and intuition to marry the two to produce a forecast. In the same way improving computational data assimilation techniques to account for errors in the locations of structures will improve the model's prediction. Tools have been developed for a forecaster to locate structures and correct their positions by hand (Hou & Strum 1999), however an objective, automated algorithm is more suited for the vast amounts of data in use today.

The causes of location errors are complicated but certainly model simplifications, discretization, poor estimates of the background error, and sparse observation in space and time play the major part (Brewster 2003). Many different methods that attempt to reduce location errors have been implemented. Mariano (1990) reduces fields to

contours, analyzes the shape and location of the contours, identifies their analogs in another field, and creates an analysis field by averaging the contours' shapes and locations. Brewster (2003) finds volumes that define analogous structures in two 3D data fields, and then searches for and implements a displacement that minimizes the error associated with them. Chen and Snyder (2007) chose to correct vortex structures by moving the location of the center of the vortex. In addition they explore correcting the shape of the vortex by correcting aspects such as major and minor axis length and rotation angle. Alexander et al. (1998) looked at a model field and an observation field then manually selected what he called "tie points" representing analogous points of structures in the different fields. He then warped the grid so that the location of the tie points in the model's field matched those in the observation field. Here we also consider grid warping, but simplify and automate the technique and study the resulting improvements in forecast error. A more sophisticated method for warping grids in two dimensions is described in Ravela et. al. (2006).

In this paper we focus on the identification and alignment of jets. In the case of jets a simple example makes it clear that alignment before interpolation is advantageous. With many accurate observations at short time intervals optimal interpolation works well, doesn't require much computational effort, and will always improve the model state. However if the model is allowed to deviate from reality interpolation begins to show its weaknesses and structures appear to be destroyed. If the distance between the locations of the observed and modeled jet centers is large then the jet produced by interpolation, referred to as the analysis jet, will be wider and weaker than the observed and modeled jets as seen in Fig. 1a. However if the jets peaks can be aligned prior to this averaging then the magnitude and width of the analysis jet is comparable to that of the observed and

modeled jets shown in Fig. 1b. This provides motivation for aligning jets before the assimilation cycle in a prognostic model.

The jet structure was chosen because it is easy to model with a simple geophysical representation and its structure information can be simplified to the location and width of the jet. However, modifications of the technique would render it applicable to vortices, fronts, and other coherent features. Jets in the atmosphere can be difficult to observe with standard methods of determining winds aloft, such as soundings, even when dealing with large scale features such as the jet stream. In reality the ability to detect the location of structures requires that the observations are fine enough to resolve them. If the observation network is not dense enough structures will be missed. This is a problem for all data assimilation methods, in that coarse observations can miss large amplitude small-scale features. In the case of the proposed algorithm, if the observations are too coarse to see a jet the algorithm merely continues without jet alignment and will not change the analysis. An advantage of this technique is that the structure's location may be determined from the data that is most suitable, including currently under-utilized information from sources such as such as satellite retrievals, radar reflectivity, and aircraft data.

In this study a standard and simple form of data assimilation is implemented and then a jet-aligning algorithm is added in order to study improvements made in forecasting skill. Section 2 gives a brief background of the data assimilation technique used in this study. The alignment technique we explore does not critically depend on this choice of data assimilation method and could be modified to work with other standard methods. Section 3 describes the algorithm used to identify and align jet structures. Section 4 describes the numerical model used in the study. Section 5 describes the experimental

procedure and evaluates the improvement in forecast skill resulting from jet alignment. Finally, conclusions are given in section 6.

2. Data Assimilation

Statistical data assimilation methods produce an analysis state using linear combinations of the model state and the observations. One simple method of data assimilation is optimal interpolation. Here, this combination is weighted using knowledge of errors in the observations and error growth in the model in the form of error covariance matrices. Error covariance matrices can be difficult to fully compute if there are many grid points in the state space as their size is the number of grid points squared. We chose to use optimal interpolation in this study because when proper assumptions are made the result is a technique with low computational cost, due to vanishing covariances, yet still similar to 3DVAR in many ways. The jet alignment technique we investigate is independent of the choice of data assimilation method and could be adapted to work with other methods as well.

Optimal interpolation uses a background state X_b and observations Y to produce an analysis state X_a by adding their weighted difference.

$$X_a = X_b + W(Y - HX_b), \tag{1}$$

$$W = BH^T(HBH^T + R)^{-1}, \tag{2}$$

Where W is a weight matrix, H is a transform from model space into observation space, B is the background error covariance matrix, and R is the observation error covariance matrix. An element of an error covariance matrix represents error at one point due to the influence of error at another point. The background error covariance matrix B includes the effects of error in the model due to discretization and faulty model physics. For

simplicity we assume that this error is spatially uncorrelated and that the background error covariance matrix B is diagonal (Parrish and Derber, 1992). We further assume that observation errors are not spatially correlated, making R diagonal. We also assume that observation errors are Gaussian perturbations of a spatially homogenous value so that R is the identity multiplied by the field's value times a constant.

The matrix B is calculated using the so-called National Meteorological Center (NMC) method (Parrish and Derber 1992; Rabier et al. 1998). To determine a 12-hour background error using this method we start with three experiments, one to represent the truth, E_t and two for accumulating error called $E_{12\mathrm{h}}$ and E_{24h}. The experiments E_t and E_{24h} are initialized with the same initial conditions and then E_{24h} is perturbed by observation error. These are then run forward in time 12 hours. The E_{12h} experiment is then set to equal to E_t at 12 hours and perturbed by the observation error. The experiments are then run for another 12 hours so that for the last twelve hours we can calculate the errors in both E_{12h} and E_{24h} denoted Err_{24h} and Err_{12h}. An ensemble of n such experiments is run, in our case we used 250. The background error is then calculated at every point i in the grid as:

$$B_i = C\sum_n (Err^i_{24\,hr} - Err^i_{12\,hr})/n \tag{3}$$

Where C is a normalization factor (Bouttier 1994) given by the ratio of the average maximum of error in a 12 hour run and the average maximum error in a 24 hour runs. The NMC method is used because errors arising at short time scales manifest at small scales, which when averaged over many runs cancel out. The NMC method looks at the

error from 12 to 24 hours, which occurs on larger scales and is more representative of the background error.

Observations are simulated by treating one of a twin pair of models as "truth". We will work with the velocity field in a quasi-geostrophic model, described in detail below. The observed velocity V_o is obtained by taking the value from the model representing truth and adding Gaussian noise. The velocity in the second model is the background velocity V_b, and the analysis velocity V_a at each grid point is the background velocity plus a weighted difference of the background and the observations:

$$V_a = V_b + (V_o - V_b) * \frac{\varepsilon_b}{(\varepsilon_o + \varepsilon_b)}, \qquad (4)$$

Where ε_o and ε_b are, respectively, the observation and background errors at the grid point. If the observation error ε_o is much larger than the background error ε_b, the analysis is approximately equal to the background; in the opposite situation the analysis is dominated by the observations.

3. Structure Alignment

To develop a data assimilation technique that can correct the locations of structures three tasks must be addressed: defining the structure in the background and observational fields, assimilating the variables that define the properties of the structure, and creating an analysis field with the modified structure. A structure identification algorithm typically produces variables describing the structure such as its location, strength, and width. Examples of such techniques are given in Davis et al. 2006 and Wernli et al. 2008. The properties of the observed and background structure can be

assimilated using any standard data assimilation technique. Here we use optimal interpolation for simplicity. Finally warping the grid produces a structure in the analysis field with the appropriate properties.

There are a variety of procedures one can use to identify structures in complex flows. Although some of these methods can be quite complex, it is often the case that very simple methods provide significant benefits. Here we use a simple one-dimensional jet identification method to demonstrate the utility of jet identification and assimilation. More complex methods such as identifying the jet using an isoline of potential vorticity (i.e. Martius et al. 2006) and then employing a two-dimensional grid warping approach were considered, however while using a more complex method is expected to lead to improvements it is unclear if these will be significant enough in this case to justify the additional computational cost. On each meridional grid line we use the one-dimensional zonal velocity to define the location and width of a possible jet on that cross-section. The maximum zonal velocity on each meridional grid line is identified as the center of the jet. The width of the jet on each meridional grid line is calculated using the standard deviation of the zonal velocity.

If the locations of the jets are the same there is no need for alignment and the process is aborted. The process is also aborted when the difference in location between the observed and background jet locations are larger than a threshold d_{max}. In this situation the background and observed jets are not interpreted as analogous features. For example, one could have a split jet, where in the observations one branch has a larger zonal velocity and is interpreted as the main jet, while in the background, the other branch has a larger zonal velocity. This situation can also arise if the background has deviated too far from truth. These situations could be treated with a more complex

algorithm but it was found that they are rare occurrences with negligible effects and the simpler method was chosen.

If analogous jets are found in the background and observations, the analysis jet location is determined using optimal interpolation. In order to accomplish this the jet location background error and the jet location observation error must be known along with the modeled and observed jet locations. The jet location background error for each longitude represents the error in jet location produced by the model at each meridional cross-section and is determined by running the model forward in time and using the NMC method described above. The jet location observation error represents the average error created in the location of the jet's maximum from the process of observing and is calculated by performing Monte Carlo runs perturbing a jet containing field with Gaussian noise equivalent to observational error. It is assumed that the observation errors are the same on each meridional slice.

The analysis jet is produced independently on each meridional grid line for which analogous jets are identified in the background and observation. The background and observed fields are each modified through grid warping to move the location of their respective jets to the analysis jet location. In order to isolate the jet from other features of the flow, which we do not want to be affected by the structure alignment procedure, grid warping is done on only a subset of the latitude range in the model. To obtain this region the observed and background jet widths are scaled by a jet width factor, $c_{width} < 1$, the resulting scaled width determines a jet region around each jet location, and the union of the background and observation jet regions determines the region over which grid warping is implemented.

In mathematical terms the grid warping is a mapping from an original space x to a warped space x^*. The warping is defined by requiring that a certain critical point x_c, in

this case the background or observed jet location, is mapped to a specific location x_c*, the analysis jet location. The boundaries of the warped region x_{min}, x_{max} remain fixed, x_{min}=x_{min}*, x_{max}=x_{max}*. Grid points between the critical point and the boundary are warped using linear interpolation, resulting in separate transformations for $x < x_c$ and $x > x_c$:

$$x^* = \left(\frac{x_c^* - x_{\min}}{x_c - x_{\min}} \right) x + \left(\frac{x_c - x_c^*}{x_c - x_{\min}} \right) x_{\min}, \qquad x_{\min} \le x \le x_c \tag{5}$$

$$x^* = \left(\frac{x_c^* - x_{\max}}{x_c - x_{\max}} \right) x + \left(\frac{x_c - x_c^*}{x_c - x_{\max}} \right) x_{\max}, \qquad x_c \le x \le x_{\max} \tag{6}$$

Values of fields $f(x)$ such as velocity are mapped so the new value at the mapped grid point is equal to the old value at the original grid point, $f^*(x^*) = f(x)$. The grid warping transformation is illustrated in Fig. 2.

The jet alignment procedure has two parameters, the maximum jet separation d_{max}, and the jet width scaling factor c_{width}. If the detected jets are separated by more than d_{max} the transform is not performed because the two jets are most likely not analogous. The algorithm was empirically found to work well with d_{max} equal to 10 grid points, which corresponds to roughly 1000 km, and c_{width} = ¾. The results were found to be fairly independent of the values of these parameters.

In general, grid warping will result in an unbalanced velocity field. Here, geostrophic balance is maintained by using the aligned velocity field to compute a vorticity field, which is then used to create a streamfunction. The streamfunction is used to evolve the system in time via the quasi-geostrophic equations described below.

4. Model Description

We test the effectiveness of jet alignment in improving forecasts using a simple two-layer quasi-geostrophic channel model with periodic boundary conditions in the zonal direction (Vautard et al. 1988; Duane and Tribbia 2004). Evolution of the potential vorticity is calculated in a pseudo-spectral code using the quasi-geostrophic potential vorticity equations

$$\frac{Dq_i}{Dt} = \frac{\partial q_i}{\partial t} + (\frac{\partial \Psi_i}{\partial x})(\frac{\partial q_i}{\partial y}) - (\frac{\partial \Psi_i}{\partial y})(\frac{\partial q_i}{\partial x}) = F_i + D_i \ , \tag{7}$$

$$q_i = \left[\nabla^2 \Psi_i + (f_0 + \beta y) + \frac{1}{R^2}(-1)^i (\Psi_1 - \Psi_2) \right] \ , \tag{8}$$

where q is the potential vorticity, which is conserved if there is no forcing or dissipation. Ψ_i is the stream function with layers i = 1, 2. The forcing F_i and dissipation D_i are

$$F_i = \mu_0 (q_i^* - q_i) \tag{9}$$

$$D_i = [(-1)^i \nu^{\text{int}} \nabla^2 (\Psi_1 - \Psi_2)] - [\delta_{i,2} \nu^{Ek} \nabla^2 (\Psi_2)] + [\alpha \frac{\partial^8 q_i}{\partial x^8} + \alpha \frac{\partial^8 q_i}{\partial y^8}] + [D_i^p] \tag{10}$$

The forcing is defined by the vorticity field q_i^*, displayed in Fig. 4, which is the state to which the model tends to relax. This shape is chosen because it is a simple way to create a constrained channel using meridional gradients in stream function and force a jet-like flow. The dissipation includes four terms which are from left to right: The friction between the layers internally, the friction at the surface or Ekman damping (note this only affects Ψ_2), hyper viscosity, and extra terms in *D* that damp the slow modes. A typical instantaneous flow field is depicted in Fig. 5, which shows a jet with a zonal wave

number near 7 and is trapped by the high gradient of potential vorticity that acts as a waveguide (Schwierz et al. 2004). The details of the model setup and parameters are discussed by Vautard and Legras (1988) and Duane and Tribbia (2004). We use a resolution of 256 by 64 grid points in the zonal and meridional directions respectively. The background error covariance obtained using the NMC method described above is shown in Fig. 6. As is evident in this figure the background error is highest near the forcing and is advected to the right with the flow.

5. Results

The jet alignment technique was tested by running three independent channel models: one to represent the truth and two for data assimilation. Of the two data assimilation channels, one is used as a control, with optimal interpolation alone, and the other tests the addition of the new jet alignment algorithm as an additional step. Error is defined as an average kinetic energy given by the RMS differences of velocities at each grid point i as:

$$Error = \sum_{i} (U_i - U_i^{'})^2 / (2i) \tag{11}$$

Where U_i and U_i' are the velocities of the models representing truth and that used for data assimilation respectively at gridpoint i. Error saturation was determined by letting two channels run independently for a long time and then computing an average inter-channel 'error'. The model is run past its transient state to obtain an initial field that is used to initialize all three channels. The initial states of the two assimilation channels are then slightly perturbed and all three channels are stepped forward in time. Every 12 hours an

observed field is generated by perturbing the 'truth' field at each grid point with Gaussian noise generated with the Box-Muller algorithm. A value of 10% of the field value is used as the standard deviation of the noise as errors in jet streaks in data sparse regions tend to be 5-9% (Cardinali et al. 2004). Assimilation is then done in the two channels using this observation field. The control field assimilates the observations using only optimal interpolation; the experimental field first aligns the modeled jet with the observed jet and then proceeds to implement optimal interpolation. The 12-hour assimilation cycle is then repeated 1000 times and the 12 hour forecast errors are collected.

The average kinetic energy of the RMS error as a function of time for a typical run (Fig. 7) shows that both data assimilation techniques consistently keep the error below the saturation point, and that there is nearly always an improvement with the jet alignment algorithm. The error through the 12-hour assimilation cycle, averaging over 1000 assimilation cycles, is shown in Fig. 8. Immediately after assimilation the error slightly decreases for roughly 1.5 hours while stable modes perturbed by the adjustment equilibrate (Lindzen and Farell, 1980). The two assimilation techniques produce similar error traits but aligning the jets prior to assimilation decreases the average error at 12 hours by 51%.

The variability in improvement is seen in the probability distribution function (PDF) of the average ratio of the kinetic energy of the error per grid point in the control assimilation to that in the jet-aligned assimilation (Fig. 9). The average value of the ratio is 3.62 indicating a clear reduction of error when using the jet aligning technique. The PDF has a long tail, indicating that in some cases the alignment technique vastly outperformed the control assimilation, however there are members of the distribution with values as low as 0.12 indicating that the jet alignment does sometimes fail and in certain cases has up to 8 times larger error. We examined some of the extreme cases and

found no clear or consistent pattern that would explain the spectacular success or failure of the method.

The above tests were done by taking observations at every grid point in the model. To test the effects of reduced observations additional experiments were performed. In experiments SG0 through SG7 observations were created at sparse locations, skipping 0 to 7 grid points respectively. The unobserved points on the grid are then filled in using cubic spline interpolation and the assimilation is done as described above. The impact of reducing observations on the effectiveness of jet alignment is shown in Fig. 10. At all observation resolutions, jet alignment has a consistent error reducing effect. The remapping process continues to show improvement even when using a spacing of 7 gridpoints in the observations because the jets are typically significantly wider than 7 grid points. As the number of observations decreases, the average ratio of the error in the control runs to the error in the jet-aligning runs decreases until the observations are so sparse that both errors near saturation (Fig. 11). The standard deviation of the ratio decreases as observation density decreases due to fewer improvements by jet alignment.

6. Discussion

We propose that data assimilation can be improved by assimilating properties of coherent structures. This idea is relevant in any data-assimilation situation and is tested here using a simple one-dimensional jet alignment technique in a two-layer QG channel. The results show that aligning structures can significantly improve a basic data assimilation method, and suggest that assimilating information about coherent structures can improve forecasts in operational numerical weather prediction. This method improves as observational information is increased and is therefore most useful with

high-resolution or high-frequency data such as that offered by radar stations and satellites.

Determining properties of structures, such as jet location, can be considered a nonlinear transformation of the field variables. Structure alignment is thus outside the scope of traditional assimilation techniques which assume linear transformations. Once one has defined a nonlinear transformation through a structure identification algorithm applied to both the observations and background, any traditional data assimilation method can be used to fix the structure property in the analysis. An inverse nonlinear coordinate transformation, implemented here by grid warping, creates a field containing a structure with the desired property. In general the difficulty of considering a full nonlinear transformation is that the space of such a transformation is too large. By focusing on the properties of coherent features, such as a jet, we eliminate this problem and obtain a specific physically motivated nonlinear transformation.

The simple algorithm presented here works independently on each meridional grid line and assumes that the jet is a single coherent streak throughout the channel. Problems can arise when the jet splits and two velocity maxima exist on a single meridional grid line. The algorithm then identifies only a single jet. If different sections of a split jet are identified in the observations and background, then the grid warping can lead to discontinuities. Adding the possibility of multiple jets to the one-dimensional algorithm would be a relatively straightforward improvement that would eliminate this problem.

Rather than improving the one-dimensional technique it might be more useful to employ two or three-dimensional mesh warping techniques similar to those used in image processing (Ravela et. al. 2007). Although these techniques are more involved and

therefore more expensive they could be worth the effort in that they can identify a wider variety of more complex structures.

The modular nature of the proposed algorithm clarifies the path to implementing structure assimilation in more realistic models, and simplifies developing and testing the steps of the algorithm. The first step is structure identification, which would probably be best accomplished with a two or three dimensional structure identification algorithm. The type of structures one wishes to align will determine which fields are used in the identification. Jets are most readily identified in the velocity field while vortices are most clearly seen in the vorticity field. Fronts might be identified using moisture, temperature and wind. Once analogous structures are identified in the model and observations, the parameters of the assimilated structure can be found using OI, as done here, or another data assimilation technique. The final step of structure assimilation is warping the background and observations to align the structures, and might be done using a multidimensional grid warping as discussed above. In more general models than those considered here, such as an operational numerical weather prediction (NWP) model like the Weather Research and Forecasting model (WRF), grid warping would destroy balances in the fields, and as part of the subsequent data assimilation of the warped fields a balancing procedure might be needed.

For instance to implement this technique to improve a WRF forecast, which is the current state of the art in operational forecasting, one might start by improving the initial condition. Typically a first guess from an operational global model such as the Rapid Update Cycle (RUC) is used in conjunction with observations to produce an analysis used to initialize the forecast. In packages such as the Local Analysis and Prediction System (LAPS) (Albers et al. 1996) a standard data assimilation scheme such as Barnes analysis, which is similar to OI but uses a radius of influence (Barnes 1964), is

used to assimilate the observations. This will cause misaligned structures such as jets to be weakened as mentioned previously. To use an alignment method here one would develop a technique to identify jets and quantify their properties using a combination of all of the available data. This would include soundings, visible and infrared satellites, aircraft measurements, etc. Once the observed structure is parameterized a shift in the model representation can be defined that will better align the structure with the truth and all modeled fields can be transformed in the same way. Warping all fields the same way will preserve some balances but ultimately this transform of the model fields will unbalance the model. This is not a large hurdle as there are many techniques and tools that will balance a set of model fields post assimilation and in fact many analysis packages such as LAPS and the Space-Time Mesoscale Analysis System (STMAS) have balancing built in (McGinley et al. 2001 and Xie et al. 2005). The improved and balanced analysis can then be used to initialize a new forecast cycle.

Acknowledgements. Throughout this study BEB was partially supported by NSF Grant ATM-0327929 and the NOAA Earth Systems Research Lab. JBW and GSD were partially supported by NSF Grant ATM-0327929. The National Center for Atmospheric Research is sponsored by the National Science Foundation.

REFERENCES

Albers S., J. McGinley, D. Birkenheuer, and J. Smart 1996: The Local Analysis and Prediction System (LAPS): Analyses of clouds, precipitation, and temperature. *Weather and Forecasting*, **11**, 273-287.

Alexander G.D., J.A. Weinman, and J.L. Schols, 1998: Use of digital warping of microwave integrated water vapor imagery to improve forecasts of marine extratropical cyclones. *Mon. Wea. Rev*., **126,** 1469-1496

Barnes, S. L., 1964: A technique for maximizing details in numerical weather map analysis. *J. Appl. Meteor*., **3**, 396-409.

Bouttier, F., 1994: A Dynamical Estimation Of Forecast Error Covariances In An Assimilation System. *Mon. Wea. Rev*., **122**, 2376-2390

Brewster K.A., 2003: Phase-correcting data assimilation and application to storm-scale numerical weather prediction. Part I: Method description and simulation testing. *Mon. Wea. Rev*., **131**, 480-492

Cardinali, C., L. Rukhovets, and J. Tenenbaum, 2004: Jet Stream Analysis And Forecast Errors Using Gads Aircraft Observations In The DAO, ECMWF, And NCEP Models. *Mon. Wea. Rev*., **132**, 764-779

Chen, Y.S., and Snyder C., 2007: Assimilating Vortex Position With An Ensemble Kalman Filter. *Mon. Wea. Rev*. **135**, 1828-1845

Davis, C., B. Brown and R. Bullock, 2006: Object-Based Verification of Precipitation Forecasts. Part I: Methodology and Application to Mesoscale Rain Areas. *Mon. Wea. Rev*. **134**, 1772-1784

Dee, D.P., and da Silva, A.M., 1998: Data assimilation in the presence of forecast bias. *Quart. J. Roy. Meteor. Soc.*, **124,** 269-296

Duane, G.S., and J.J. Tribbia, 2004: Weak Atlantic-Pacific teleconnections as synchronized chaos. . *J. Atmos. Sci.,* **61,** 2149-2168

Hou, Z., and S. Strum, 1999: Brutal but effective data assimilation for convective weather. Preprints, *Third Conf. on Coastal Atmos. And Oceanic Prediction Process, Amer. Meteor. Soc*., 297-284

Hoffman R.N., Z. Liu, J.F. Louis, et al., 1995: Distortion representation of forecast errors. *Mon. Wea. Rev*. **123**, 2758-2770

Koch, P., H. Wernli and H. C. Davies, 2006: An event-based jet-stream climatology and typology. *Int. J. Climatology*, **26**, 283-301

Lawson, W.G., J.A. Hansen, 2005: Alignment Error Models and Ensemble-Based Data Assimilation. *Mon. Wea. Rev*., **133**, 1687-1709

Lindzen, R.S. and B. Farrell, 1980: A Simple Approximate Result for the Maximum Growth Rate of Baroclinic Instabilities. *J. Atmos. Sci.,* **37**, 1648-1654

Matyas, C., 2007: Quantifying the shapes of US landfalling tropical cyclone rain shields. *Professional Geographer,* **59**, 158-172

Mariano, A.J., 1990: Contour analysis - a new approach for melding geophysical fields. *J. Atmos. &* Oceanic Tech. **7**, 285-295

Martius, O., C. Schwierz, and H.C. Davies, 2006: A refined Hovmöller diagram. *Tellus A.* **58**, 221-226

McGinley, J.A. and J.R. Smart, 2001: On providing a cloud-balanced initial condition for diabatic initialization. *Preprints, 18th Conf. on Weather Analysis and Forecasting*, Ft. Lauderdale, FL, Amer. Meteor. Soc.

Nehrkorn, T., R.N. Hoffman, C. Grassotti, et al., 2003: Feature Calibration and Alignment To Represent Model Forecast Errors: Empirical Regularization. *Quart. J. Roy. Meteor. Soc.*, **129**, 195-218

Parrish D.F., and J.C. Derber, 1992: The National-Meteorological-Centers Spectral Statistical-Interpolation Analysis System. *Mon. Wea. Rev*., **120**, 1747-1763

Rabier F., A. McNally, E. Andersson, et al., 1998: The ECMWF implementation of three-dimensional variational assimilation (3D-Var). II: Structure functions *Quart. J. Roy. Meteor. Soc.*, **124,** 1809-1829

Ravela, S., Emanual, K., and McLaughlin, D., 2007: Data assimilation by field alignment. *Physica D: Nonlinear Phenomenon,* **230,** 127-145

Schwierz, C.,S. Dirren, and H.C. Davies, 2004: Forced Waves On A Zonally Aligned Jet Stream. *J. Atmos. Sci.,* **61**, 73-87

Vautard, R., B. Legras, and M. Deque, 1998: On the Source of Midlatitude Low-Frequency Variability 1. A Statistical Approach to Persistence. *J. Atmos. Sci*., **45**, 2811-2843

Wernli, H., M. Paulat, M. Hagen, C. Frei, 2008: SAL – a novel quality measure for the verification of quantitative precipitation forecasts. *Mon. Wea. Rev.* **136**, 4470-4487

Xie, Y. F., S. E. Koch, J. A. McGinley, S. Albers, and N. Wang, 2005: A sequential

variational analysis approach for mesoscale data assimilation. Preprints, *21st Conf. on Weather Analysis and Forecasting/17th Conf. on Numerical Weather Prediction,* Washington, DC, Amer. Meteor. Soc., 15B.7. [Available online at http://ams.confex.com/ams/pdfpapers/93468.pdf.]

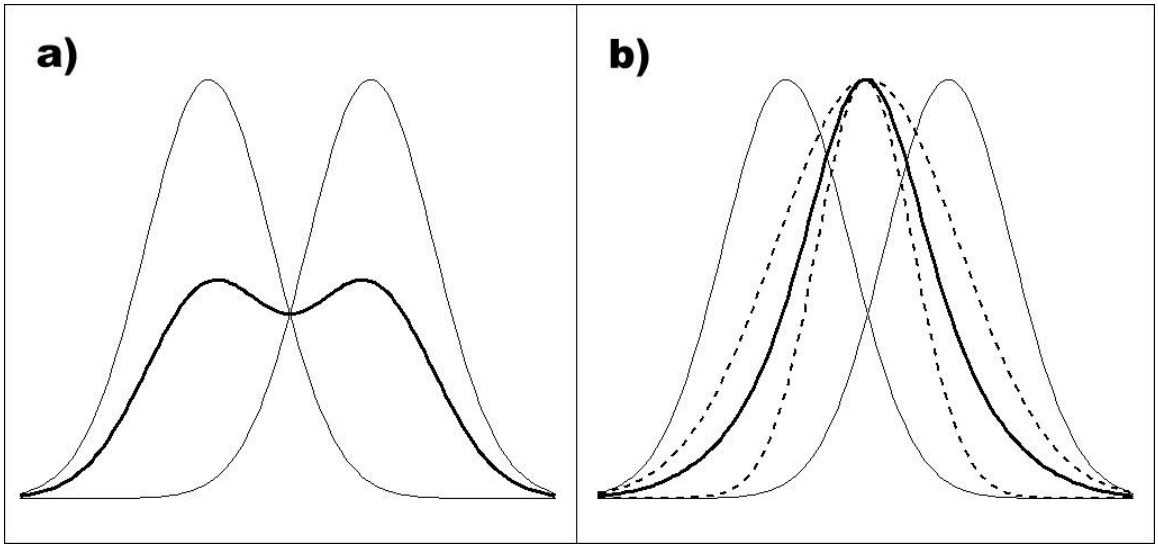

Figure 1: (a) Optimal interpolation of two fields containing jets (thin) into an analysis field (thick). Notice that the resulting structure is not only different in magnitude but is also qualitatively different in that it is wider and may have two peaks. (b) Assimilation of two jets (thin) which are first warped so that their peaks have the same location (dotted) and then assimilated into an analysis jet which retains the magnitude and shape of the original jets (thick).

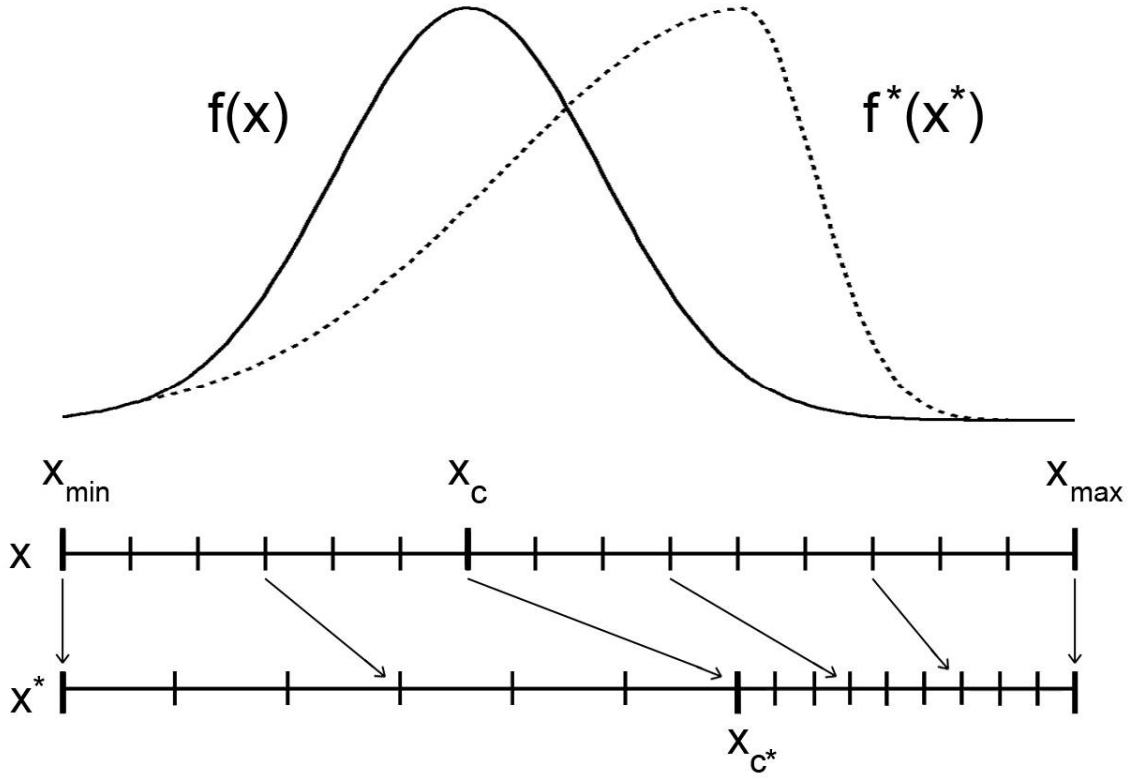

Figure 2: Idealization of the grid warping procedure. The dashed line is the result of mapping the peak of the background jet in solid black located at x_c to the analysis jet location x_{c*}.

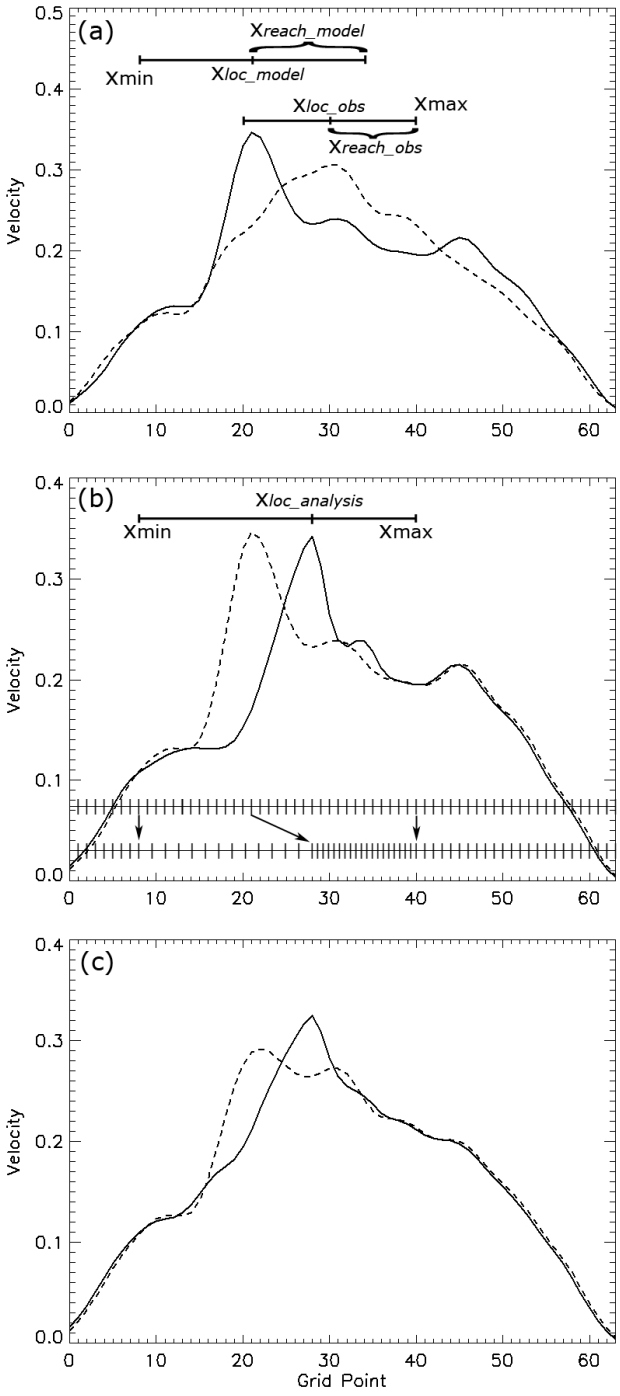

Figure 3: Illustration of the grid warping process on model data. (a) shows the velocity profile of the model (solid) and the observations (dashed) and the jet locations (x_{loc_model} and x_{loc_obs}) and jet widths (x_{reach_model} and x_{reach_obs}) associated with them. Note that the union of the spaces spanned by the jet widths is bounded by x_{min} and x_{max}. (b) is similar to Fig. 2 and depicts the warping of the model's velocity profile (dashed transformed to solid) to realign the jet's location to $x_{loc\_analysis}$. The original (top) and warped (bottom) grids are also shown. Note that this process is also applied to the observed velocity profile but is not shown here for clarity. Finally (c) shows the velocities resulting from the control technique (dashed) and the jet-aligning one (solid). In this case the correction has improved the location of the solution and preserved the structure's unimodal nature.

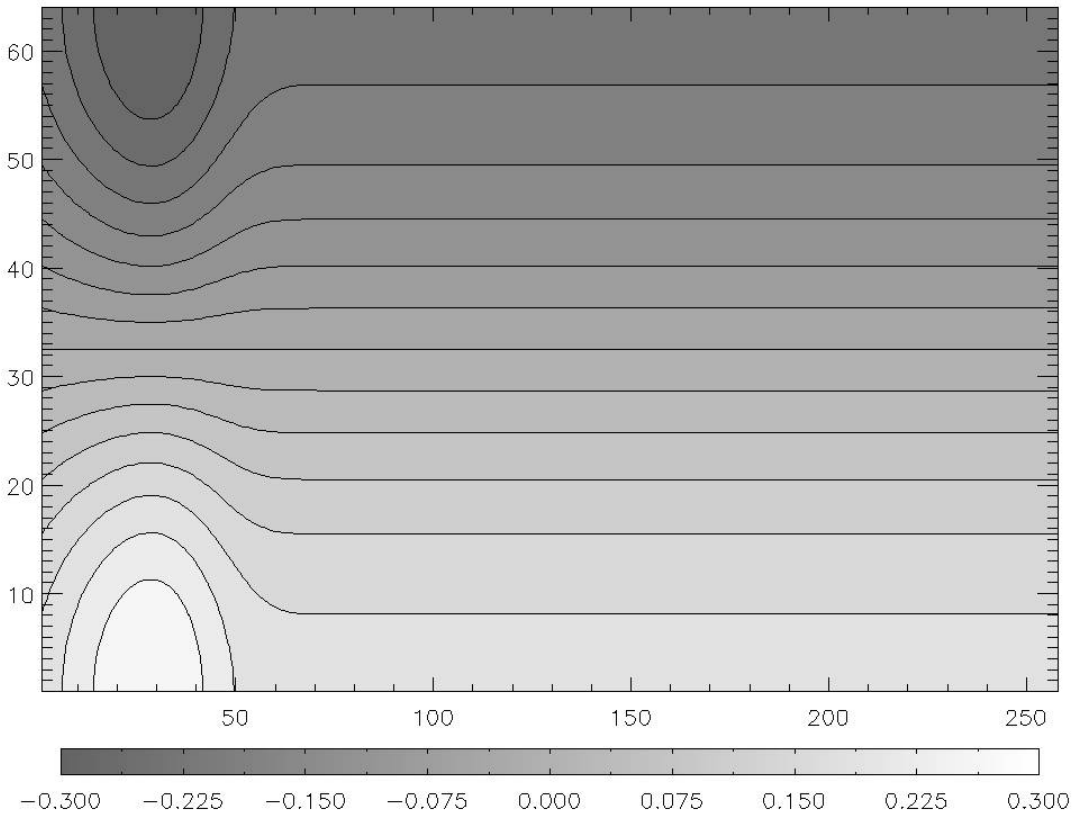

Figure 4: Horizontal cross-section of the stream function of the forcing field at midlevel in units of 1.48 x 10^9 m^2s^{-1}.

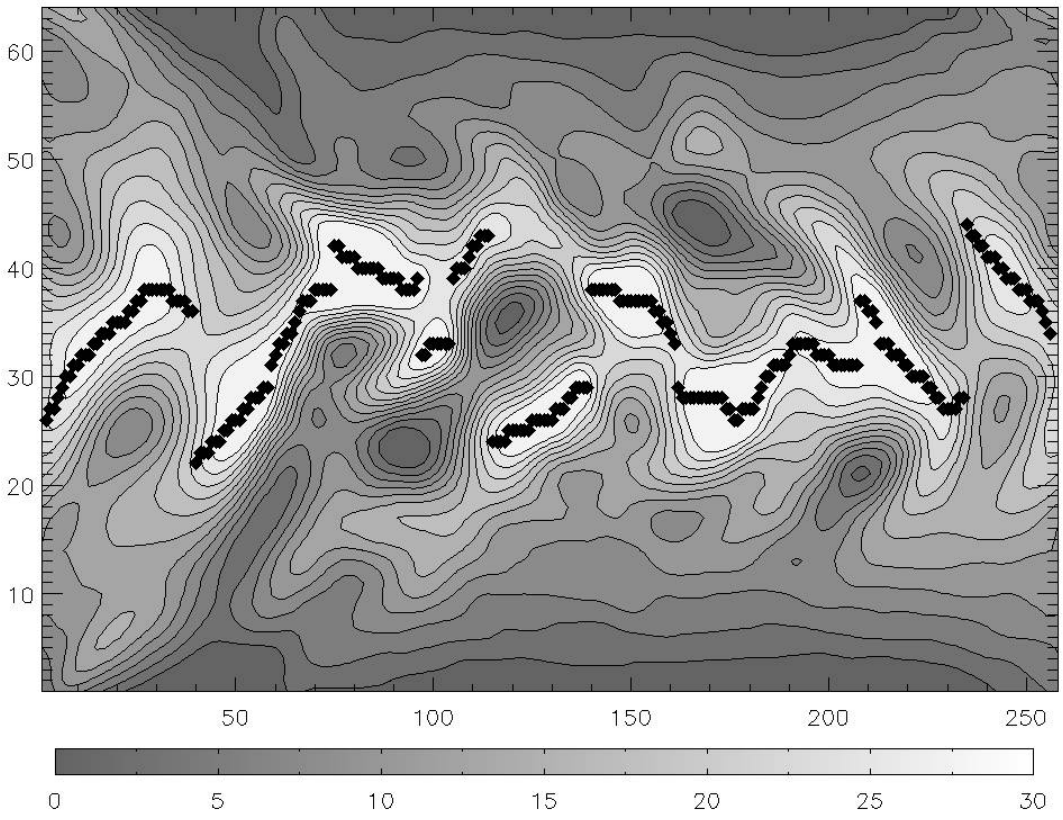

Figure 5: Horizontal cross-section of a typical instantaneous zonal velocity at midlevel in m/s. The maximum zonal velocity of the meridional cross-sections is highlighted in black. Notice the split jet in the center.

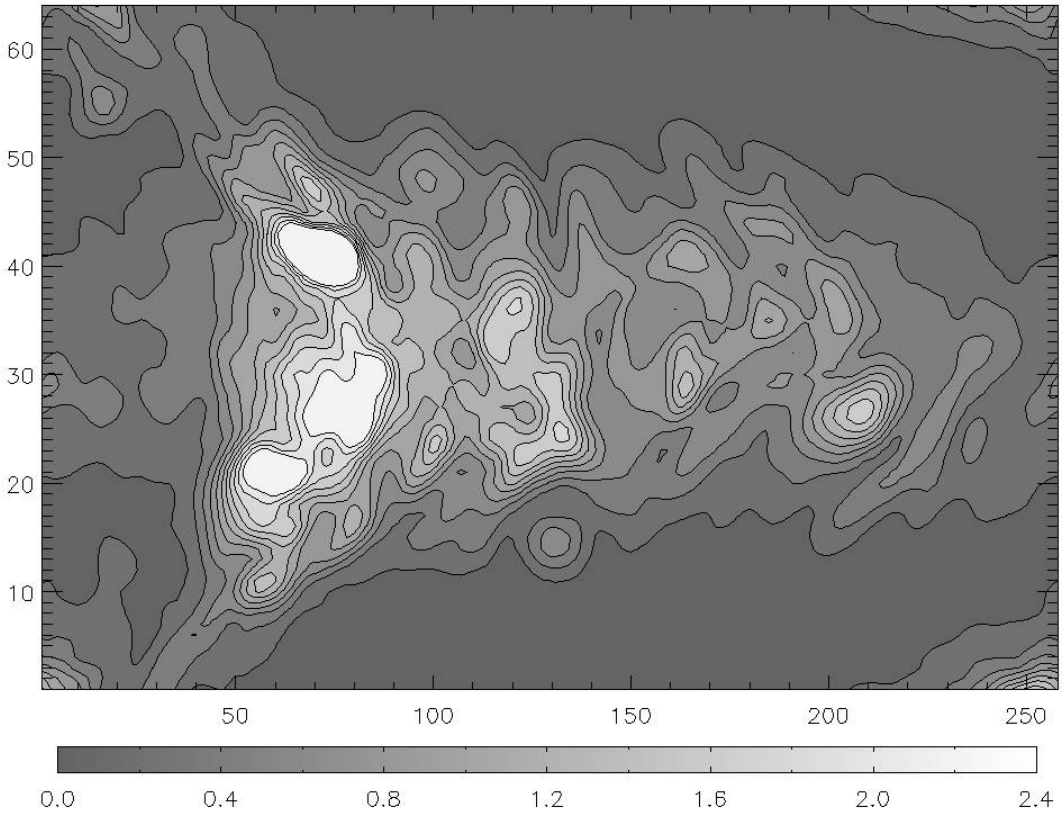

Figure 6: Horizontal cross-section of the background error covariance of the zonal velocity at midlevel in m/s.

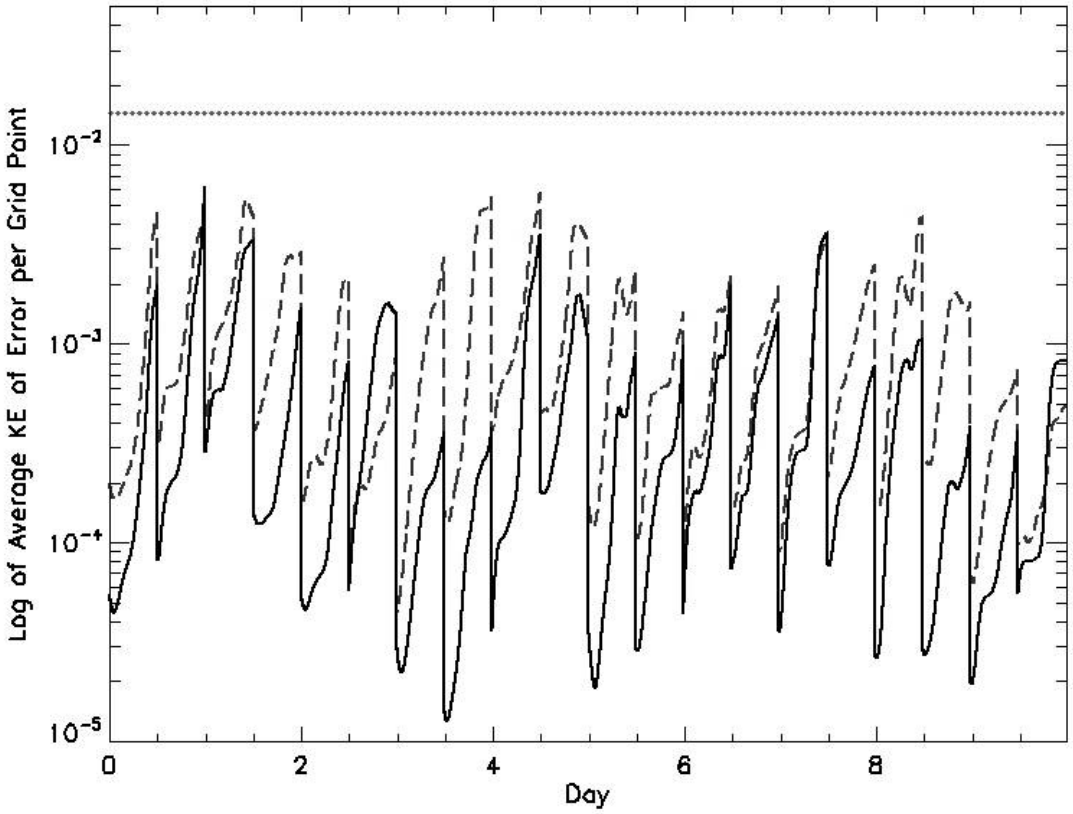

Figure 7: A typical week of assimilations as error (equation 11) versus time. The dotted horizontal line is error saturation, the dashed line is the control run and the solid line is the jet-aligning run. Note that the jet-aligning run typically has less error but occasionally has more error, such as the end of day 2.

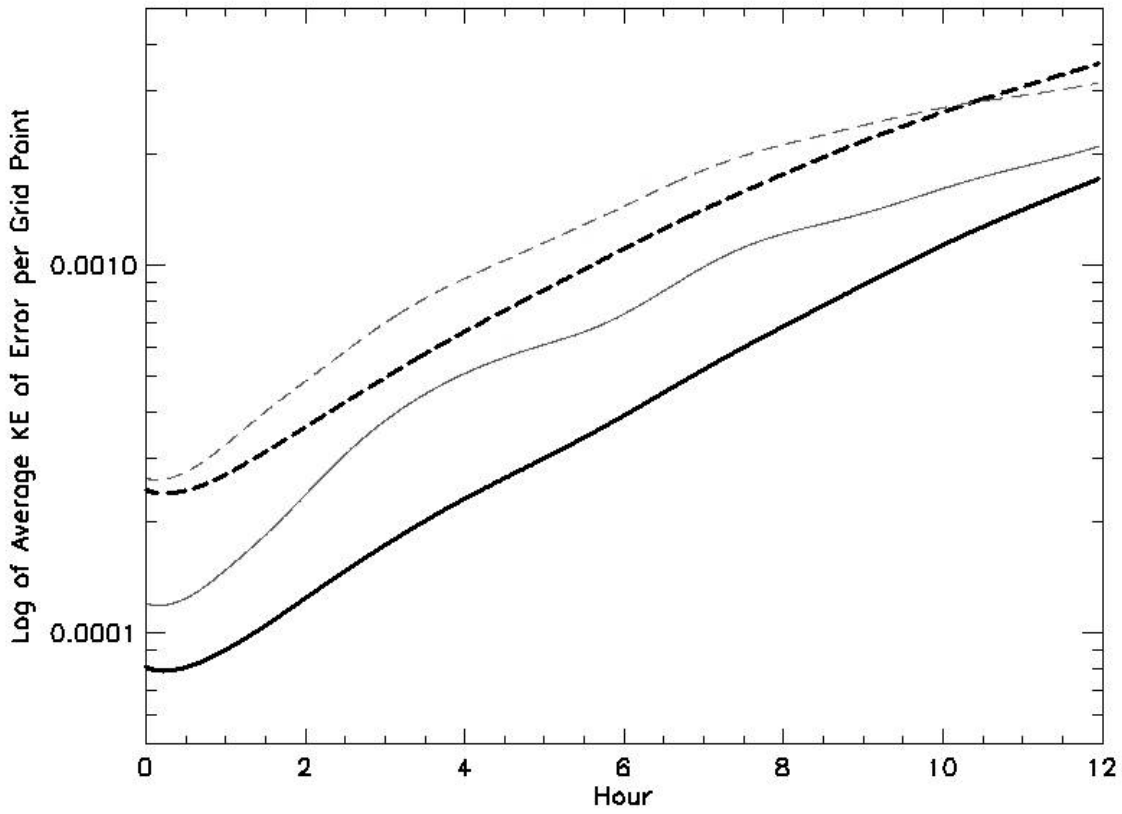

Figure 8: The average error for a 12-hour assimilation cycle averaged over an ensemble of 1000 cycles. The dashed line represents the control run and the solid line shows the jet-aligning method. The thin grey lines denote the standard deviations.

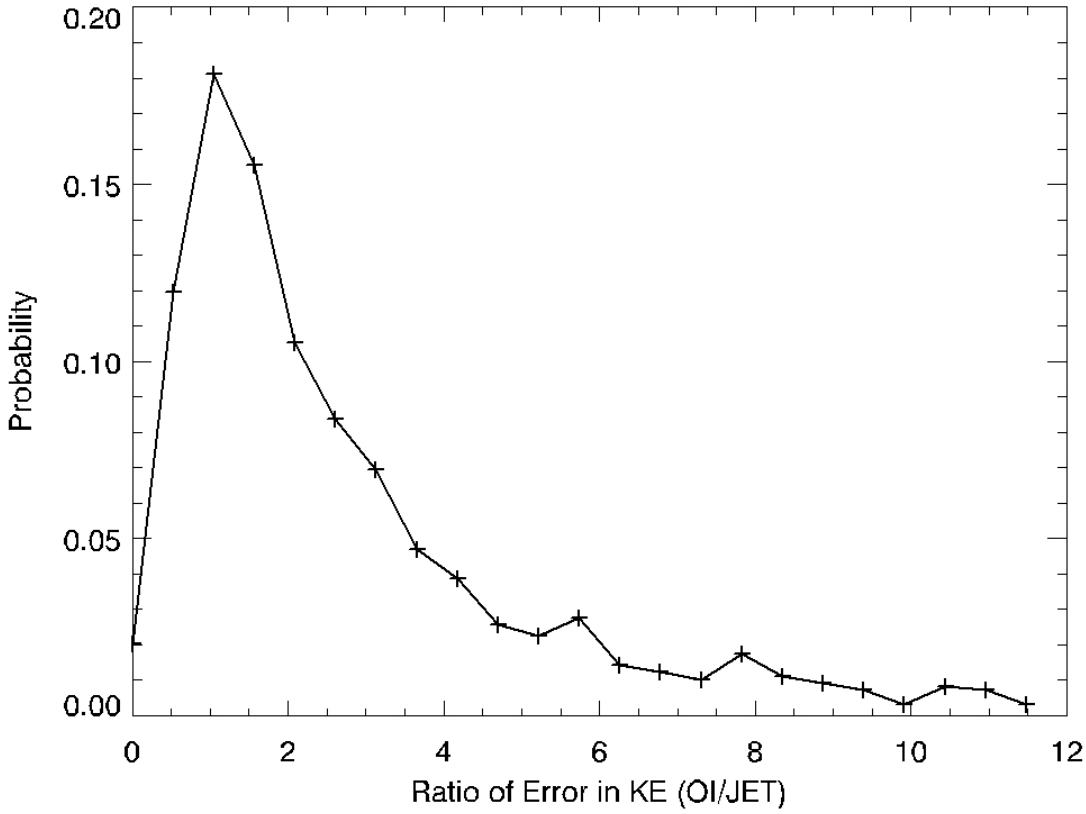

Figure 9: The probability distribution function of the ratio of error of the control assimilation to the jet-aligned assimilation at time 12 hours (1000 samples). The tail of this distribution has been truncated for the purposes of the diagram. The mean is 3.62, the median is 2.3, the standard deviation is 4.02, and the minimum and maximum values of the sample are 0.12 and 55.25.

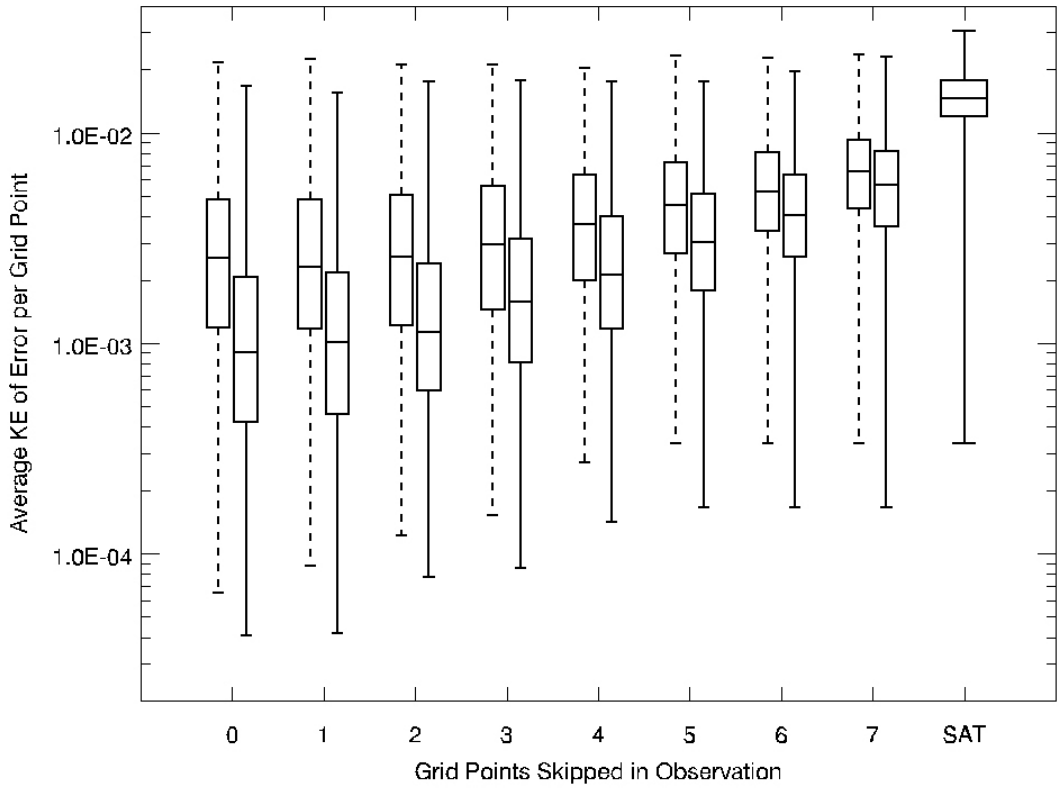

Figure 10: The range of the KE of the error, the expected value, and the range of the median 50% of the data for each experiment. The jet-aligned (solid) groups have consistently lower error than the control runs (dashed). Also as the number of observations is reduced the error increases, note that as one makes fewer observations the quality of the forecasts becomes poor and the error nears saturation (SAT).

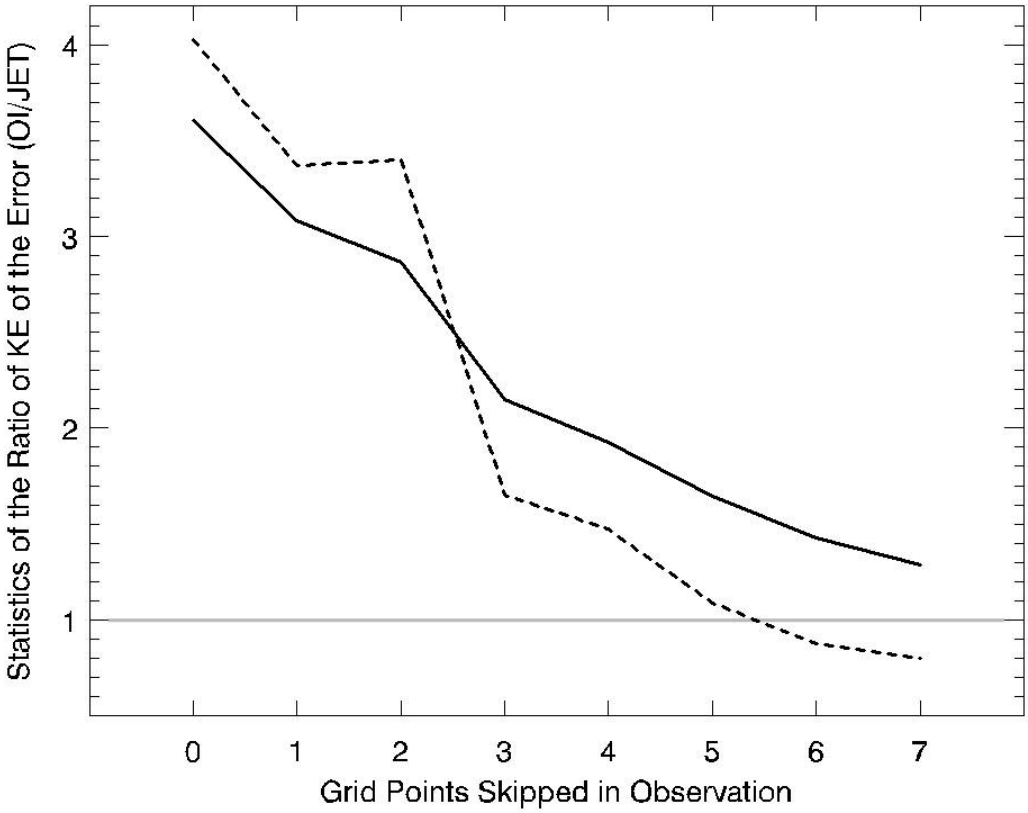

Figure 11: The average ratio of KE of the error in the control runs to the error in the jet-aligning runs at 12 hours (solid) and the standard deviation of the ratio (dashed) as a function of the number of grid points skipped in the observation. There is marked improvement up to 4 skipped grid points, where both forecasts begin to become poor and the improvement levels off.

Figure 1: (a) Optimal interpolation of two fields containing jets (thin) into an analysis field (thick). Notice that the resulting structure is not only different in magnitude but is also qualitatively different in that it is wider and may have two peaks. (b) Assimilation of two jets (thin) which are first warped so that their peaks have the same location (dotted) and then assimilated into an analysis jet which retains the magnitude and shape of the original jets (thick).

Figure 2: Idealization of the grid warping procedure. The dashed line is the result of mapping the peak of the background jet in solid black located at x_c to the analysis jet location x_{c*}.

Figure 3: Illustration of the grid warping process on model data. (a) shows the velocity profile of the model (solid) and the observations (dashed) and the jet locations (x_{loc_model} and x_{loc_obs}) and jet widths (x_{reach_model} and x_{reach_obs}) associated with them. Note that the union of the spaces spanned by the jet widths is bounded by x_{min} and x_{max}. (b) is similar to Fig. 2 and depicts the warping of the model's velocity profile (dashed transformed to solid) to realign the jet's location to $x_{loc\_analysis}$. The original (top) and warped (bottom) grids are also shown. Note that this process is also applied to the observed velocity profile but is not shown here for clarity. Finally (c) shows the velocities resulting from the control technique (dashed) and the jet-aligning one (solid). In this case the correction has improved the location of the solution and preserved the structure's unimodal nature.

Figure 4: Horizontal cross-section of the stream function of the forcing field at midlevel in units of 1.48×10^9 $m^2 s^{-1}$.

Figure 5: Horizontal cross-section of a typical instantaneous zonal velocity at midlevel in m/s. The maximum zonal velocity of the meridional cross-sections is highlighted in black. Notice the split jet in the center.

Figure 6: Horizontal cross-section of the background error covariance of the zonal velocity at midlevel in m/s.

Figure 7: A typical week of assimilations as error (equation 11) versus time. The dotted horizontal line is error saturation, the dashed line is the control run and the solid line is the jet-aligning run. Note that the jet-aligning run typically has less error but occasionally has more error, such as the end of day 2.

Figure 8: The average error for a 12-hour assimilation cycle averaged over an ensemble of 1000 cycles. The dashed line represents the control run and the solid line shows the jet-aligning method. The thin grey lines denote the standard deviations.

Figure 9: The probability distribution function of the ratio of error of the control assimilation to the jet-aligned assimilation at time 12 hours (1000 samples). The tail of this distribution has been truncated for the purposes of the diagram. The mean is 3.62, the median is 2.3, the standard deviation is 4.02, and the minimum and maximum values of the sample are 0.12 and 55.25.

Figure 10: The range of the KE of the error, the expected value, and the range of the median 50% of the data for each experiment. The jet-aligned (solid) groups have consistently lower error than the control runs (dashed). Also as the number of

observations is reduced the error increases, note that as one makes fewer observations the quality of the forecasts becomes poor and the error nears saturation (SAT).

Figure 11: The average ratio of KE of the error in the control runs to the error in the jet-aligning runs at 12 hours (solid) and the standard deviation of the ratio (dashed) as a function of the number of grid points skipped in the observation. There is marked improvement up to 4 skipped grid points, where both forecasts begin to become poor and the improvement levels off.